

超伝導量子ビットと共振器の強結合

Yasunobu Nakamura

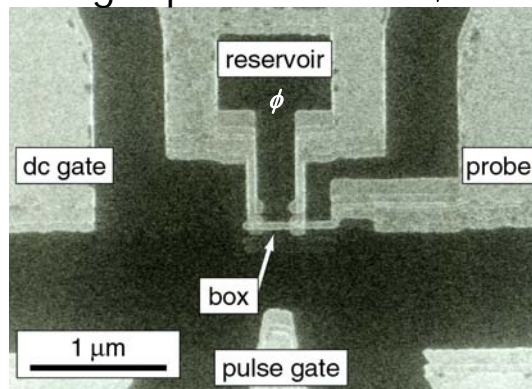
RIKEN Advanced Science Institute

NEC Green Innovation Research Laboratories

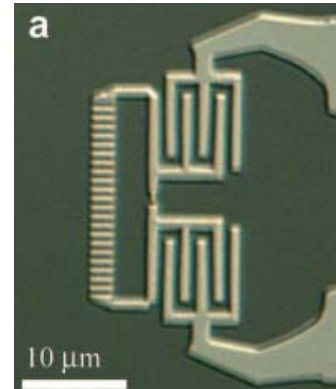


Superconducting qubits – macroscopic artificial atom in circuits

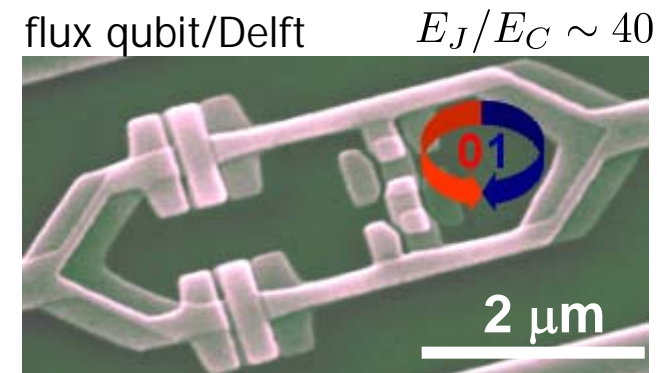
charge qubit/NEC $E_J/E_C \sim 0.3$



"fluxonium"/Yale

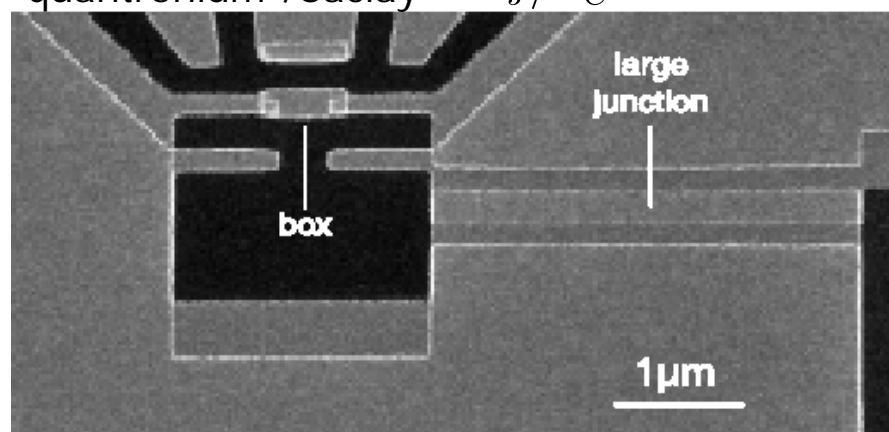


flux qubit/Delft



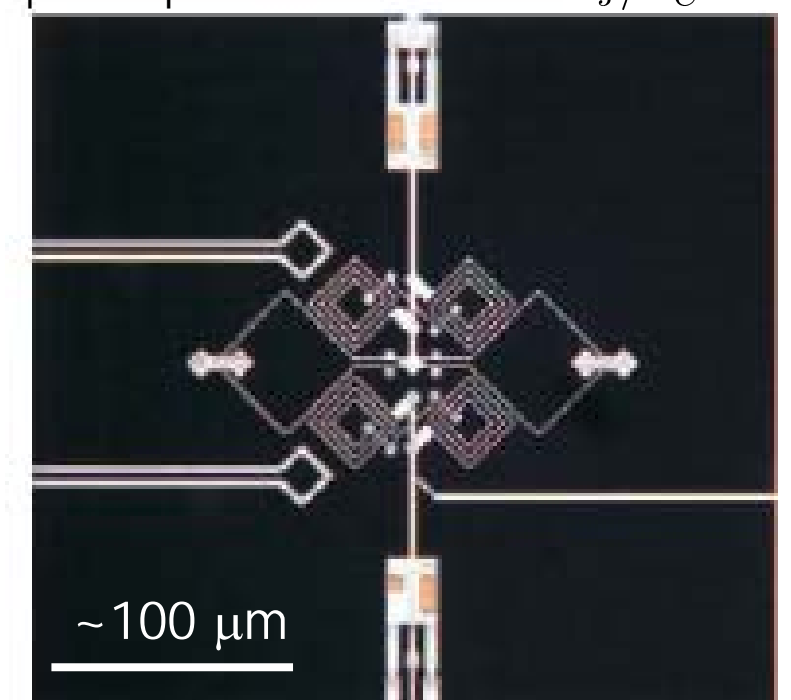
$E_J/E_C \sim 40$

"quantronium"/Saclay $E_J/E_C \sim 5$



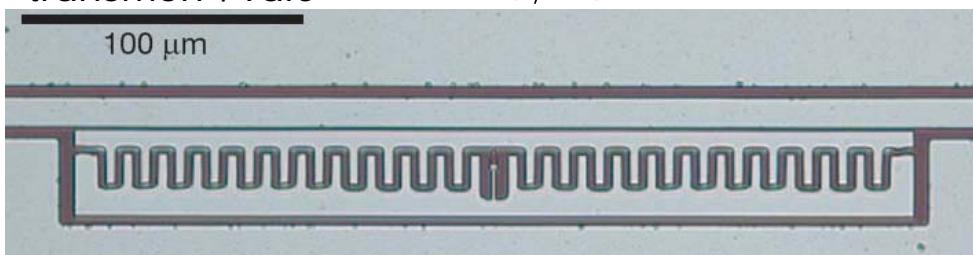
$E_J/E_C \sim 3$

phase qubit/NIST/UCSB



$E_J/E_C \sim 10^4$

"transmon"/Yale



$E_J/E_C \sim 50$

Superconducting qubits/circuits

Cons:

- Low energy photons (microwave \sim 1-10 GHz)
- Low temperature (\sim 10 mK) required
- Limited coherence time (typically \sim 1 μ s)
- Vulnerable to optical photons — quasiparticle excitations

Superconducting qubits/circuits

Pros:

- Small dissipation
- Large nonlinearity of Josephson junctions
- High-fidelity quantum circuits
 - Deterministic and fast single-qubit and two-qubit gates
 - Single-shot readout
 - On-chip multi-qubit scalability
 - Flexible design — qubits, resonators, transmission lines
 - Well-developed microwave and cryogenic engineering
- Large dipole moment
 - Strong coupling to EM modes/charges/spins/NEMS
- Improved coherence time ($\sim 10\text{-}100 \mu\text{s}$)
- Squeezing/parameteric amplification
- Single photon source/detector

Strong coupling between a flux qubit and a superconducting resonator via capacitance

Kunihiro Inomata^a

Tsuyoshi Yamamoto^{a,b}, Yasunobu Nakamura^{a,b}
and Jaw-Shen Tsai^{a,b}

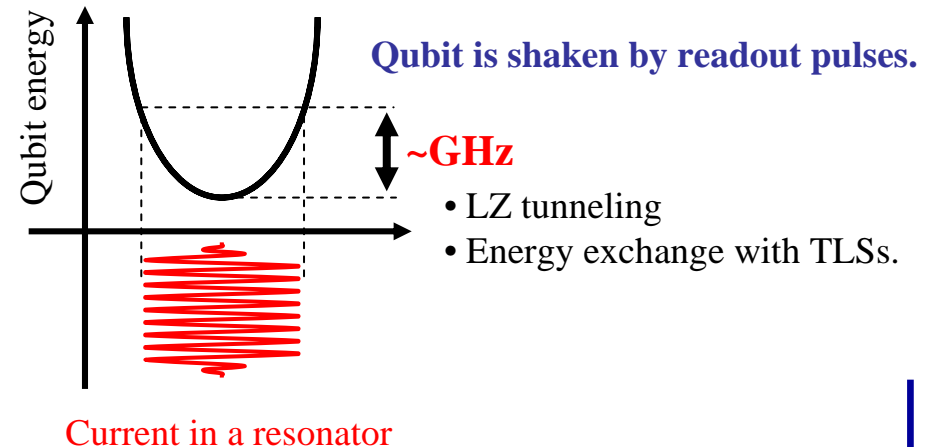
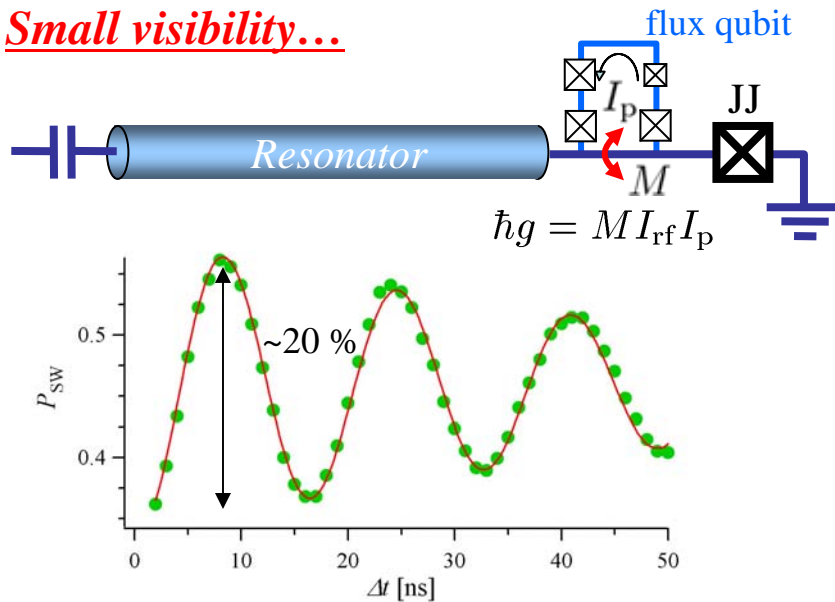
Poster No.7

a: Advanced Science Institute, RIKEN
b: Green Innovation Research Labs., NEC

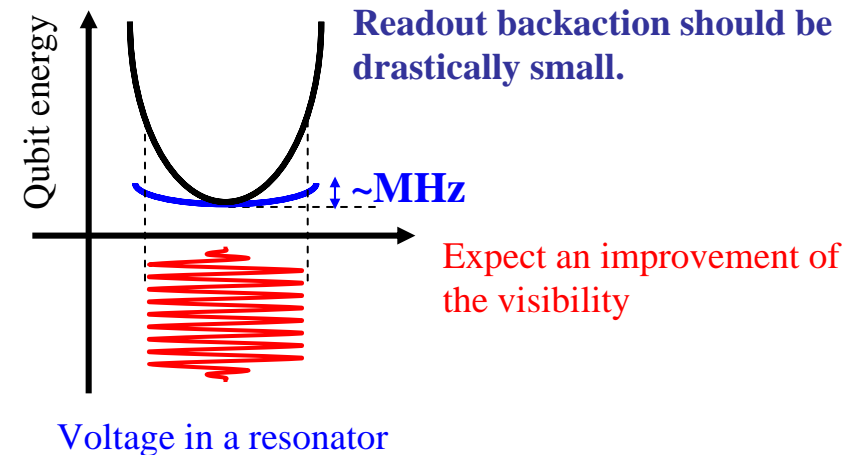
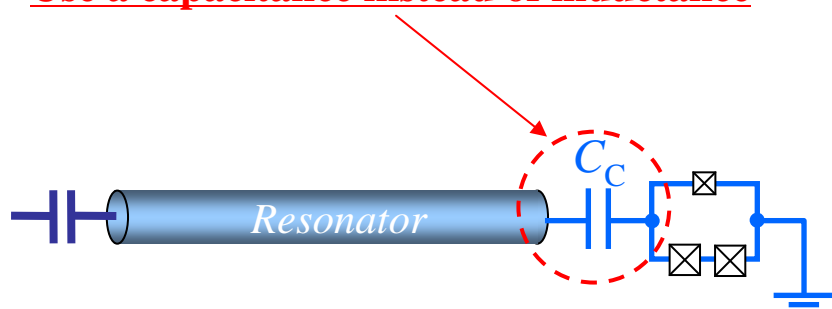


Motivation

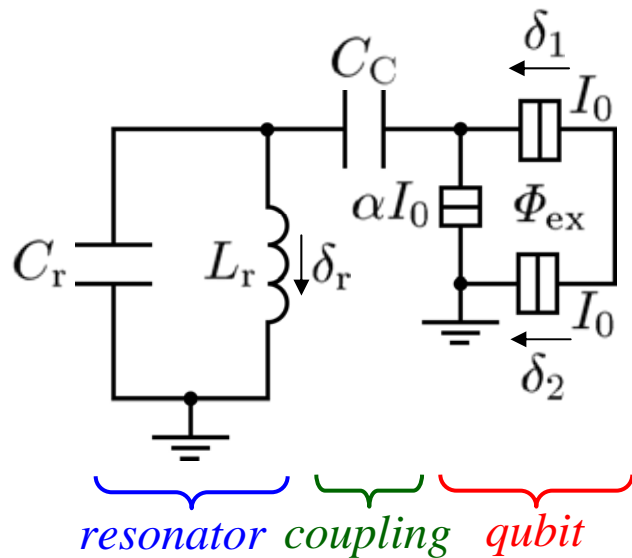
Small visibility...



Use a capacitance instead of inductance



Flux qubit capacitively coupled to a LC resonator



Circuit diagram

$\delta_1, \delta_2, \delta_r$: Phase differences

I_0 : Critical current of a larger JJ

Φ_{ex} : External flux bias

C_C : Coupling capacitor

C_r : Resonator capacitor

L_r : Resonator inductor

Total Hamiltonian of this system

$$\mathcal{H} = \mathcal{H}_q + \mathcal{H}_r + \mathcal{H}_c.$$

↑ ↑ ↑
 qubit resonator coupling

$$\begin{aligned} \mathcal{H}_q &= 4E_c \frac{1 + \alpha + \beta}{1 + 2\alpha + 2\beta} (n_1^2 + n_2^2) + 8E_c \frac{\alpha + \beta}{1 + 2\alpha + 2\beta} n_1 n_2 \\ &\quad - E_J \cos \delta_1 - E_J \cos \delta_2 - \alpha E_J \cos(\delta_1 - \delta_2 + 2\pi f) \end{aligned}$$

$$\mathcal{H}_r = \frac{E_r}{\sqrt{1+\gamma}} (a^\dagger a + \frac{1}{2})$$

$$\mathcal{H}_c = \frac{2i}{1+2\alpha+2\beta} \sqrt{\frac{\beta\gamma}{(1+\gamma)^{3/2}}} \sqrt{E_r E_c} (n_1 - n_2) (a^\dagger - a)$$

$$\beta = C_c/C_J$$

$$\gamma = C_c/C_r$$

$$E_r = \hbar/\sqrt{L_r C_r}$$

Dispersive shift in Jaynes-Cummings Hamiltonian

Jaynes-Cummings Hamiltonian

$$\mathcal{H}_{JC} = \hbar \frac{\omega_a}{2} \sigma_z + \hbar \omega_r (\hat{a}^\dagger \hat{a} + 1/2) + \hbar g (\hat{a} \sigma^+ + \hat{a}^\dagger \sigma^-)$$

In the dispersive limit, $g \ll |\omega_a - \omega_r|$ ($= |\Delta|$)

$$\begin{aligned}\mathcal{H}_{JC} &\sim \hbar (\omega_r + \underline{\frac{g^2}{\Delta}} \sigma_z) (\hat{a}^\dagger \hat{a} + 1/2) + \hbar \omega_a \sigma_z / 2 \\ &\equiv \chi\end{aligned}$$

Effective resonant frequency of the resonator

$$\omega_r - \frac{g^2}{\Delta} \quad \text{for qubit } |g\rangle$$

$$\omega_r + \frac{g^2}{\Delta} \quad \text{for qubit } |e\rangle$$

Generalized Jaynes-Cummings model

$$\mathcal{H} = \hbar \sum_j \omega_j |j\rangle\langle j| + \hbar\omega_r \hat{a}^\dagger \hat{a} + \hbar \sum_{i,j} g_{ij} |i\rangle\langle j| (\hat{a} + \hat{a}^\dagger)$$

In the dispersive limit, $g_{ij} \ll |\omega_{ij} - \omega_r|$, ($\omega_{ij} = \omega_j - \omega_i$)

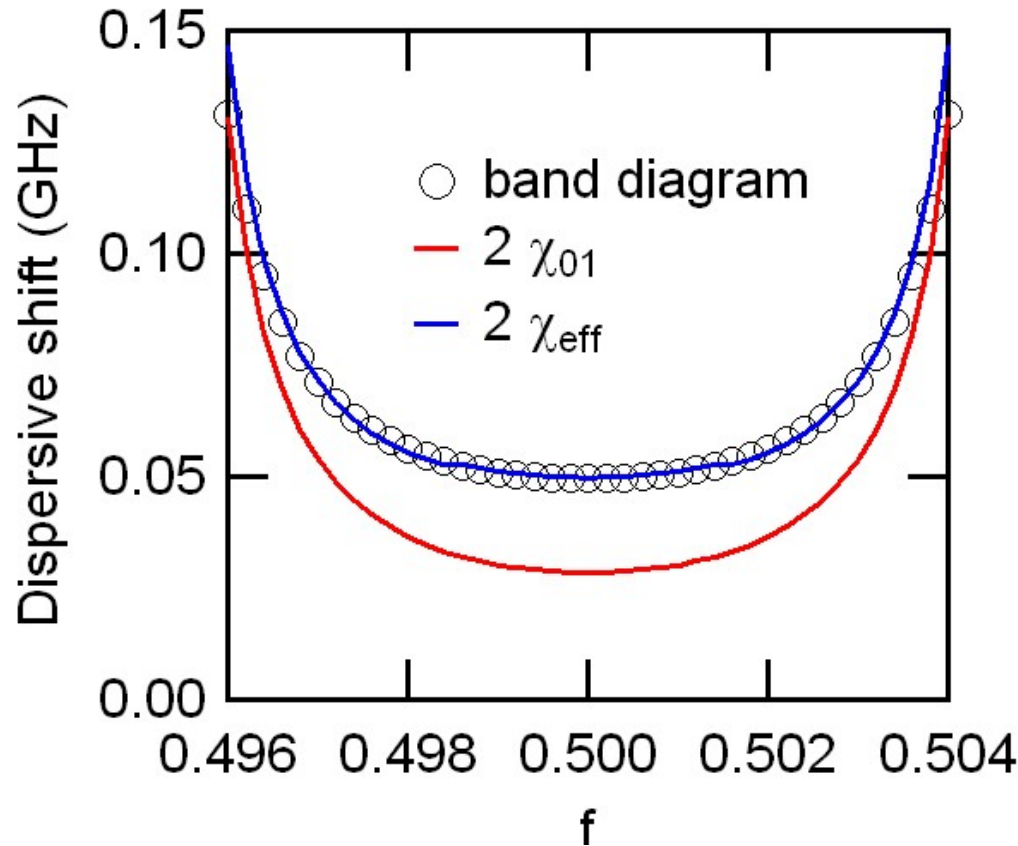
$$\mathcal{H}_{\text{eff}} = \hbar(\omega'_r + \chi_{\text{eff}} \sigma_z) \hat{a}^\dagger \hat{a} + \hbar\omega'_{01} \sigma_z / 2$$

$$\chi_{\text{eff}} = \chi_{01} - \chi_{10} + \frac{1}{2} \sum_{j=2} \left(\chi_{j1} - \chi_{1j} - \chi_{j0} - \chi_{0j} \right)$$

effect of higher states

$$\chi_{ij} = \frac{g_{ij} g_{ji}}{\omega_{ij} - \omega_r}, \quad g_{ij} = \langle i | \mathcal{H}_c | j \rangle$$

Dispersive shift

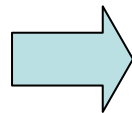


$$\chi_{\text{eff}} = \chi_{01} - \chi_{10} + \frac{1}{2} \sum_{j=2}^4 (\chi_{j1} - \chi_{1j} - \chi_{j0} - \chi_{0j})$$

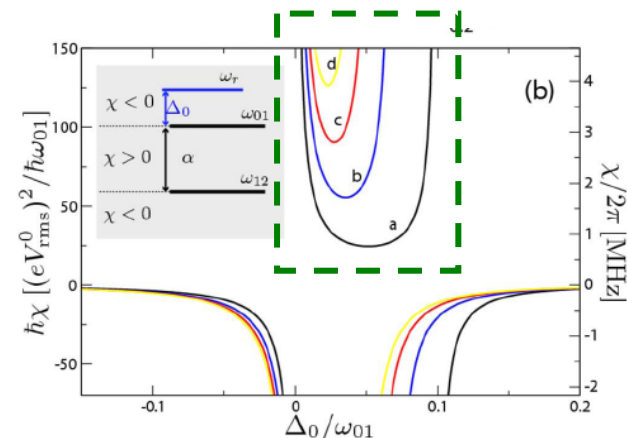
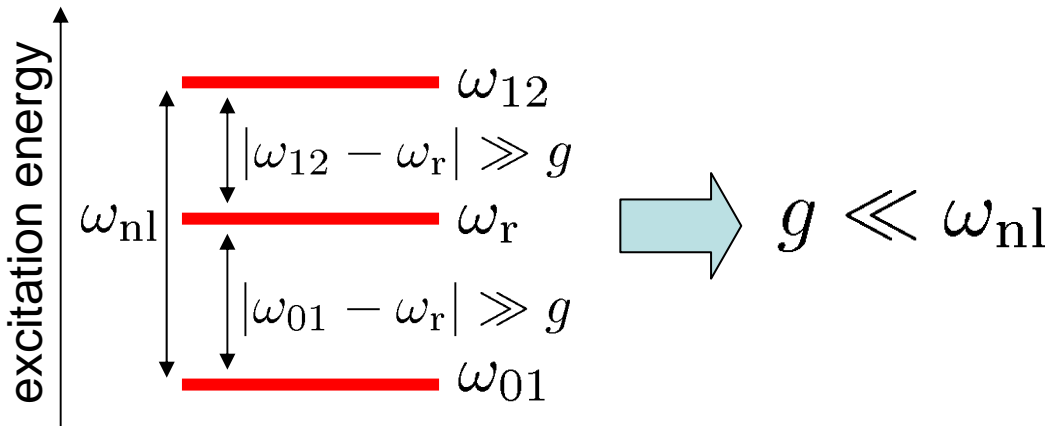
“Straddling” regime

$$\chi_{\text{eff}} = \chi_{01} + \frac{1}{2}(\chi_{21} - \chi_{12})$$

$$\chi_{ij} = \frac{-|g_{ij}|^2}{\omega_{ij} - \omega_r}, \quad \omega_{ij} = \omega_j - \omega_i$$



$\omega_{01} < \omega_r < \omega_{12}$
required condition

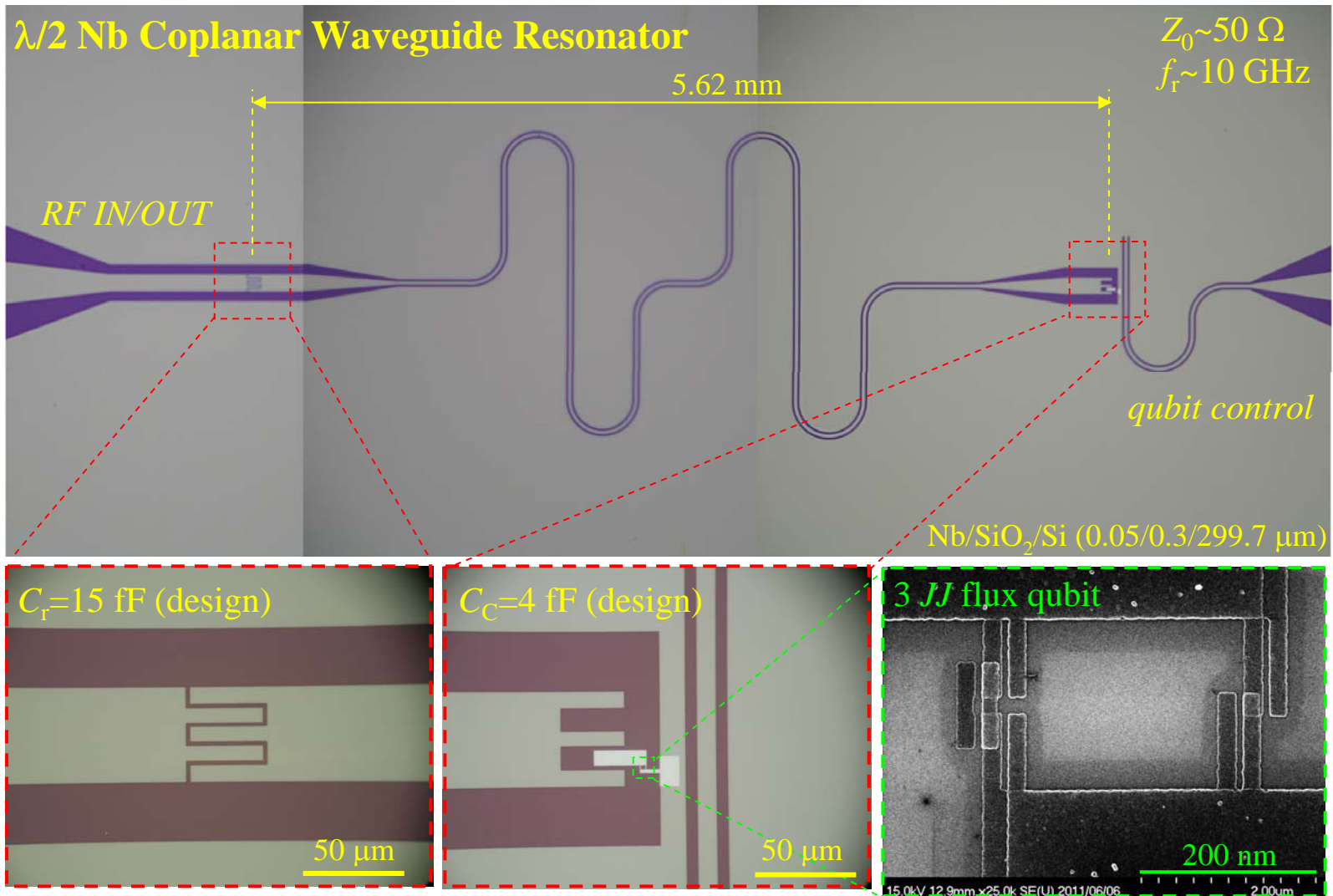


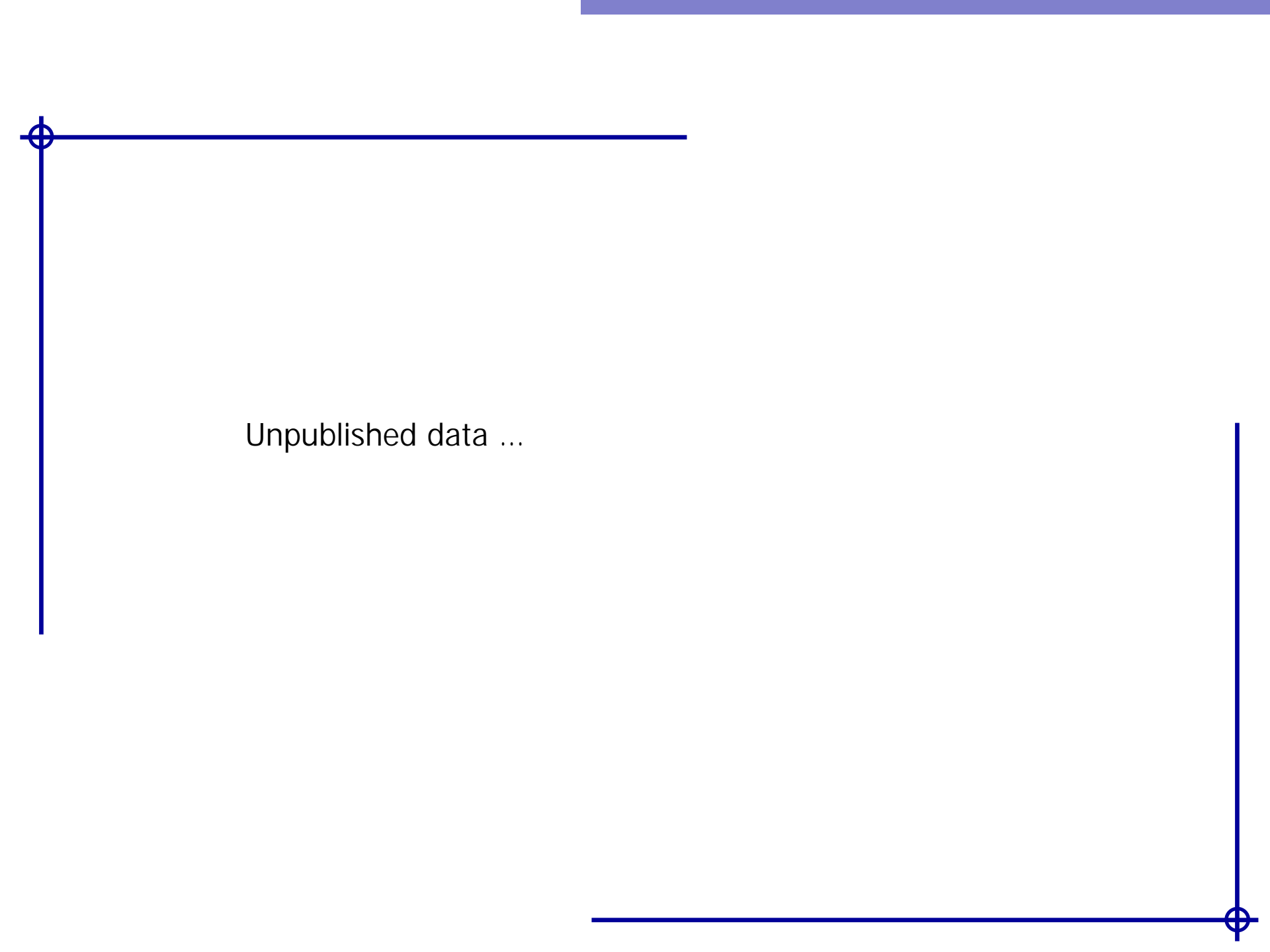
cf. transmon

Koch *et al.*, PRA **76**, 042319 (2007)

transmon
 $\omega_{\text{nl}} \sim 100 \text{ MHz}$
 flux qubit
 $\omega_{\text{nl}} \sim 10 \text{ GHz}$

Sample Images





Unpublished data ...

Superconducting qubits with epitaxial junctions

In collaboration with H. Terai, Qiu Wei, Zhen Wang (NICT)

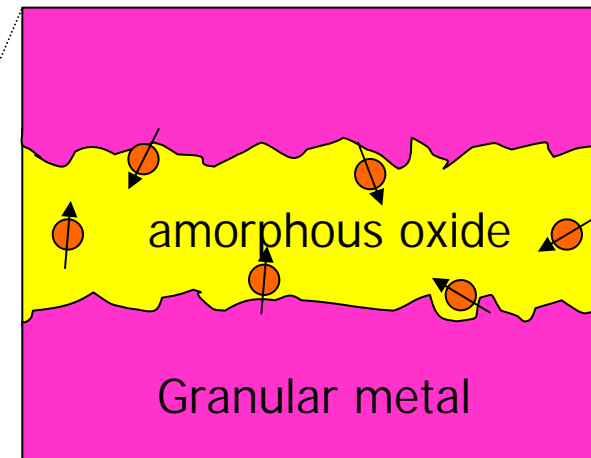
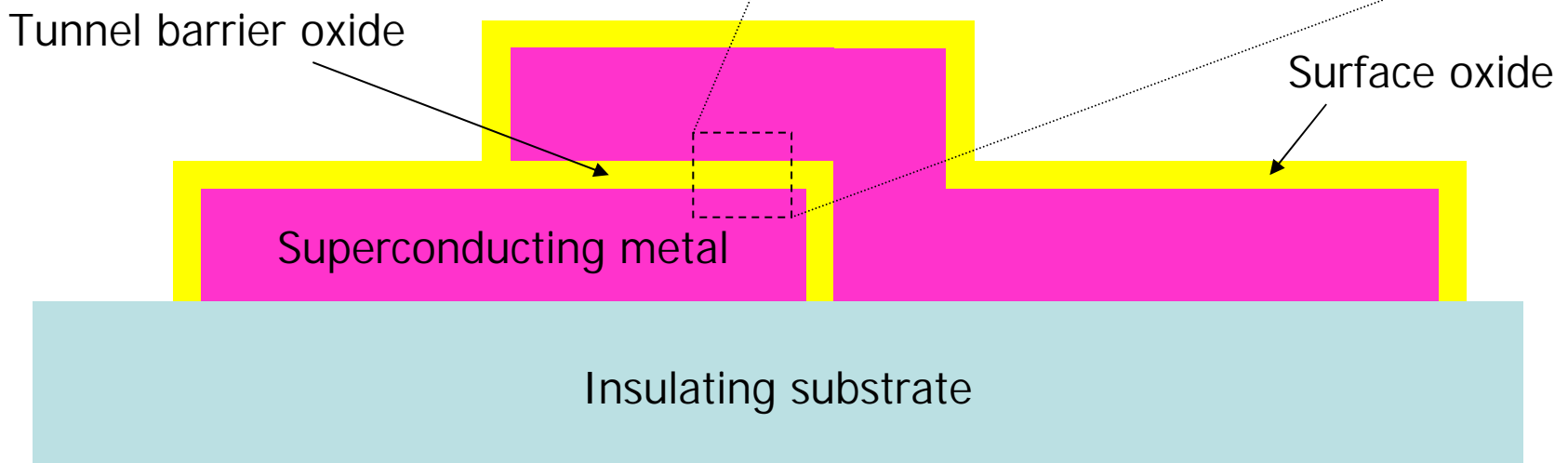
Amorphous oxides in the barrier, on the surface

Charge fluctuations

Josephson-energy fluctuations

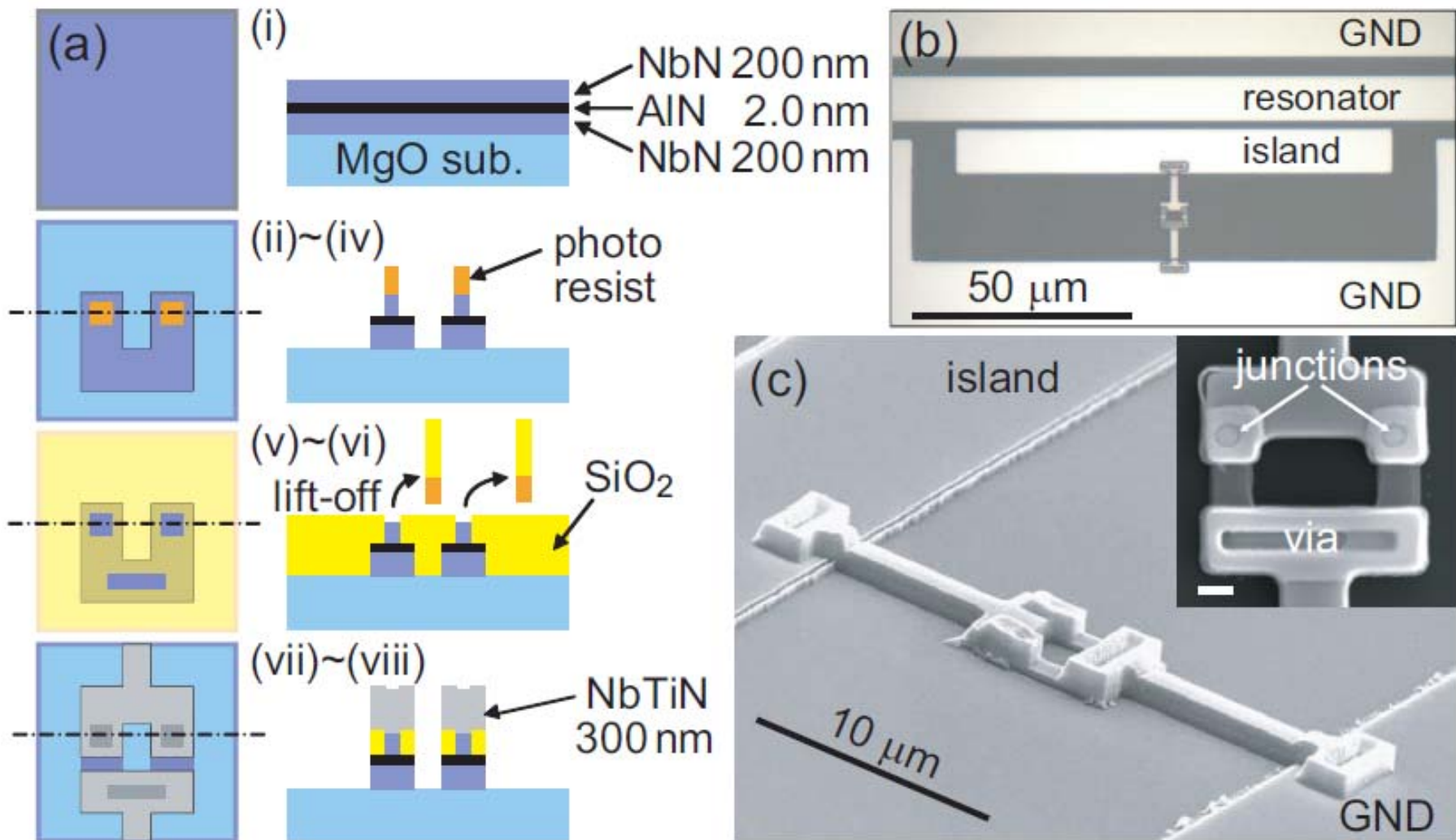
Paramagnetic spin fluctuations

{ Surface oxide
 Barrier oxide
 Metal-oxide interface

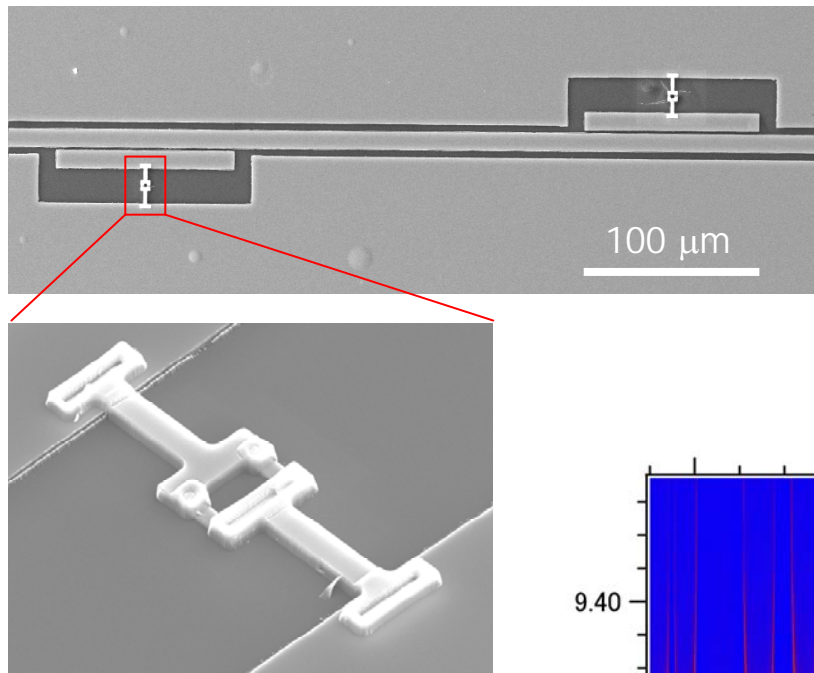


Transmon qubit fabrication

Hirotaka Terai (NICT)

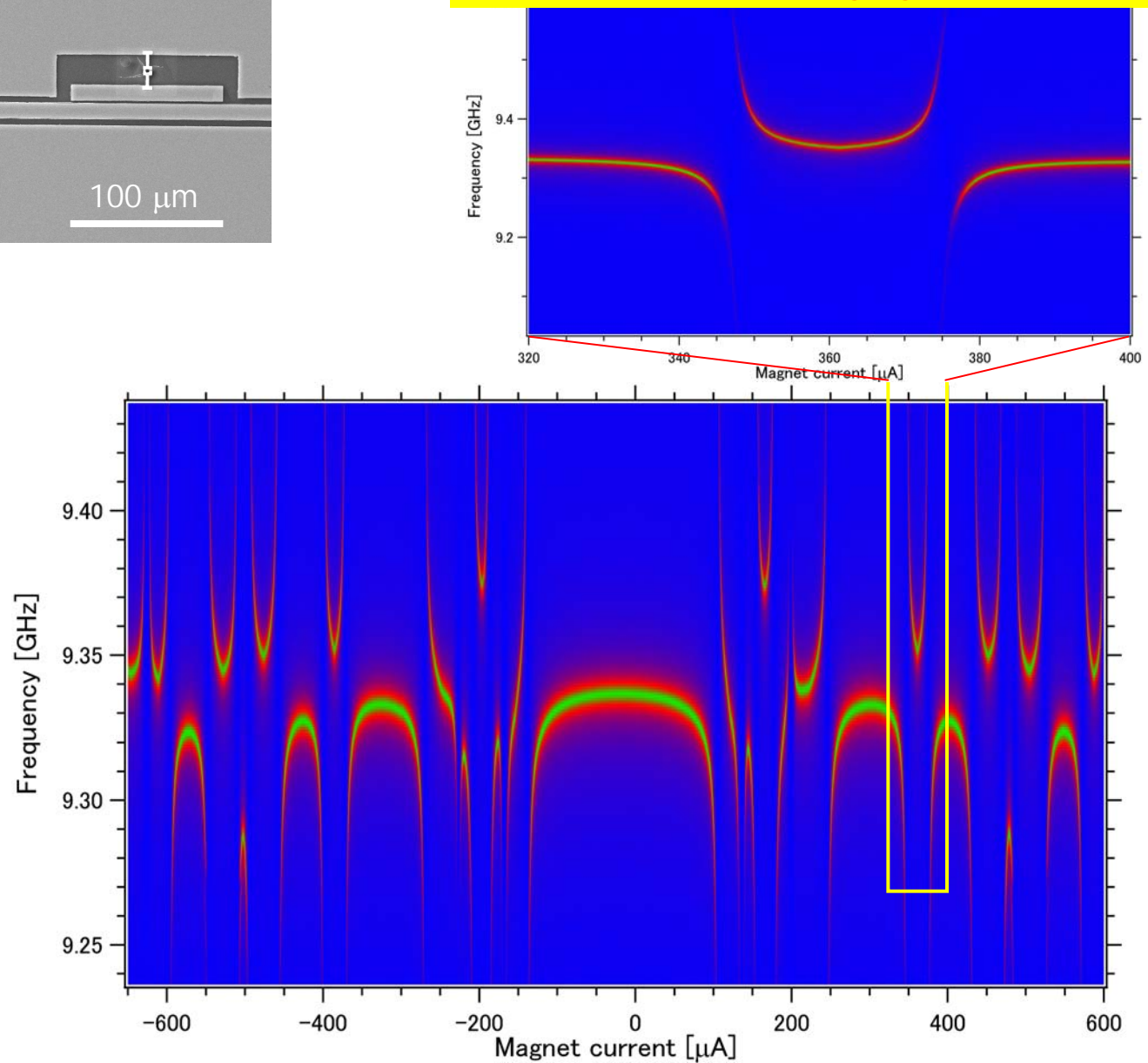


Vacuum Rabi splitting

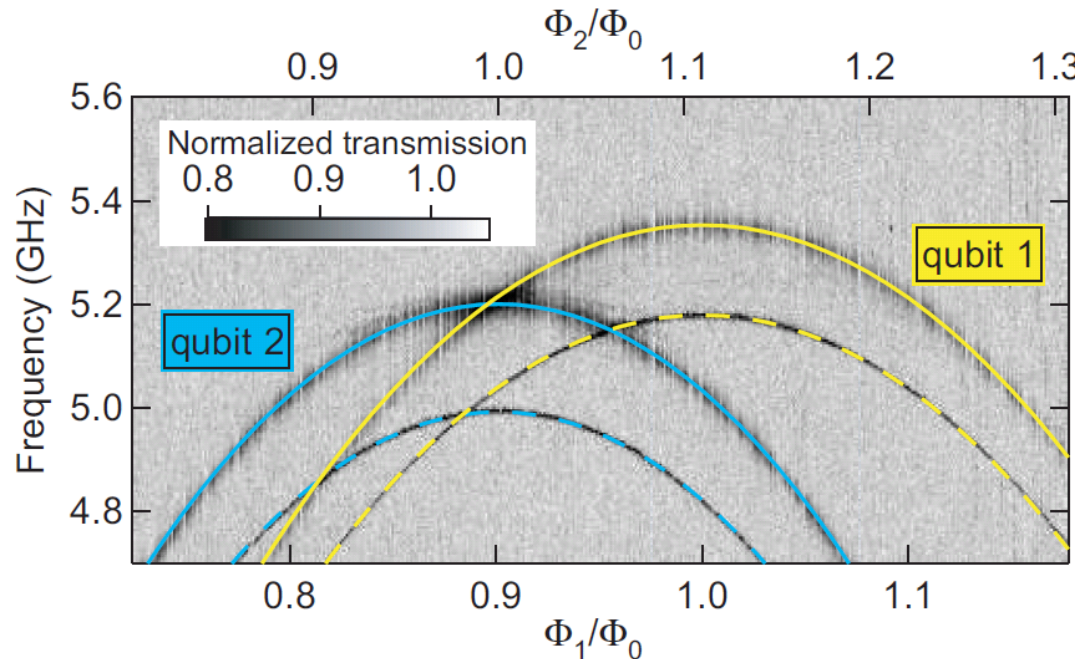


4 transmons coupled
with a resonator

Vacuum Rabi splitting: $g/h \sim 150 \text{ MHz}$



Qubit spectroscopy & decoherence time

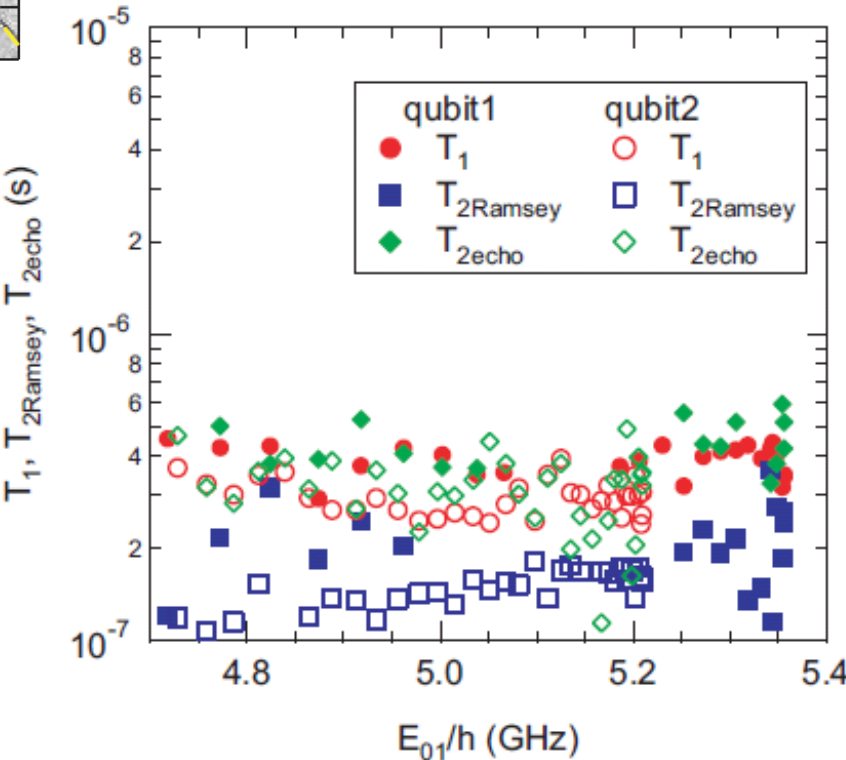
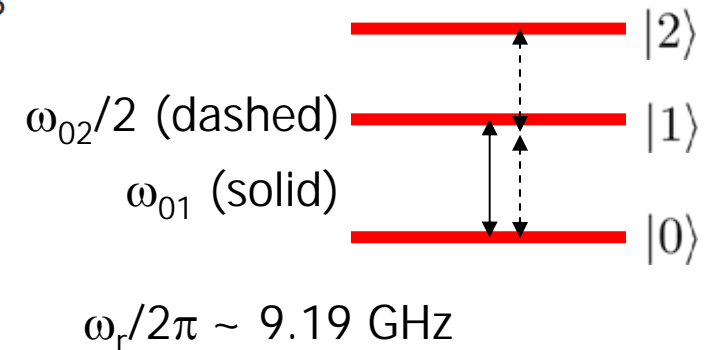


qubit 1: $E_J/h = 13.4$ GHz, $E_C/h = 0.30$ GHz

qubit 2: $E_J/h = 11.7$ GHz, $E_C/h = 0.34$ GHz

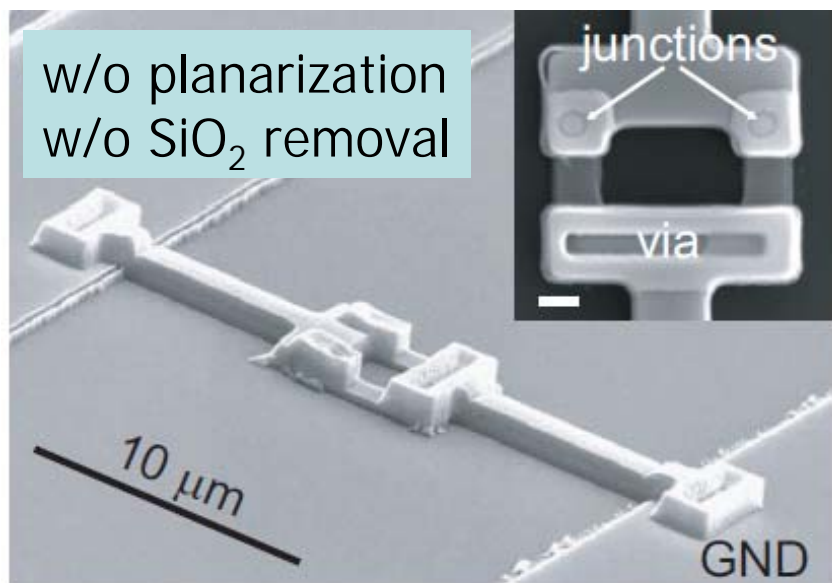
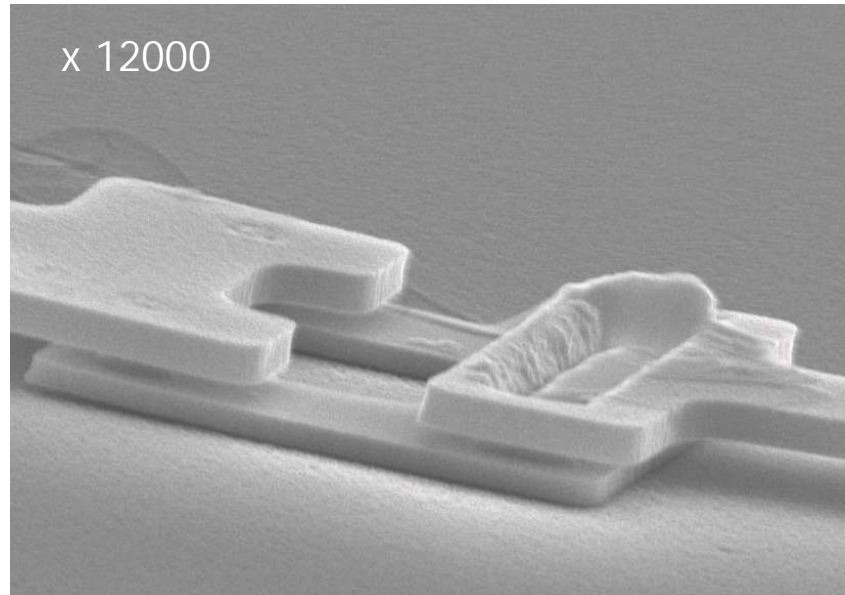
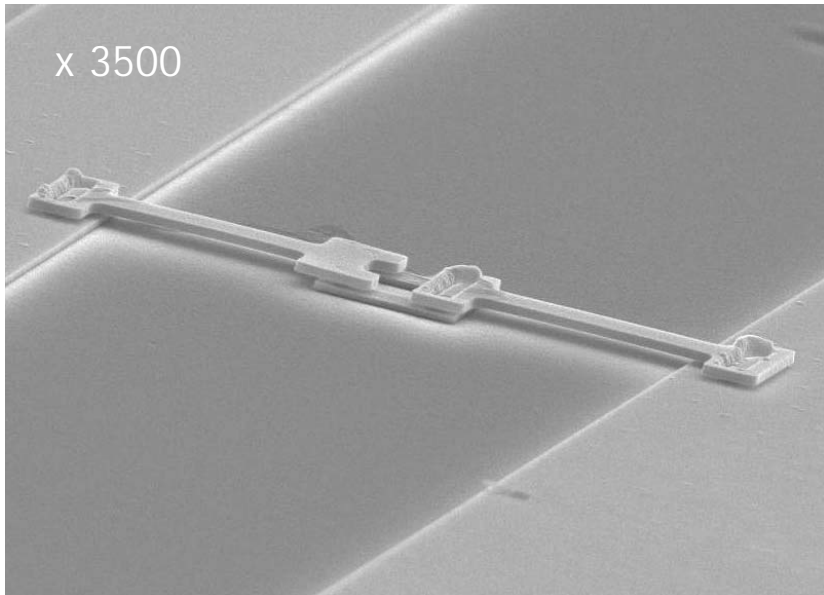
qubit-cavity coupling: $g/h \sim 0.17$ GHz

T_1	$\sim 250\text{-}450$ ns
$T_{2\text{Ramsey}}$	$\sim 100\text{-}300$ ns
$T_{2\text{echo}}$	$\sim 200\text{-}600$ ns



Planarization and SiO₂ removal

H. Terai (NICT)



To be clarified:

- Defect density in the junctions
- Effect of dielectric removal
- Smaller junctions by e-beam lithography
- Dielectric loss of MgO substrate
- Other choice of substrate